Implications of recent asperity failures and aseismic creep for time-dependent earthquake hazard on the Hayward fault

Manoochehr Shirzaei[1,2], Roland Bürgmann[2] and Taka'aki Taira[2]

[1]School of Earth and Space Exploration, Arizona State University, Tempe, AZ 85287-6004,
[2]Department of Earth and Planetary Science, University of California, Berkeley, California

Correspondence: shirzaei@asu.edu, Tel: +1 480 727 4193, fax: +1 480 965 8102

Abstract

The probability of large seismic events on a particular fault segment may vary due to external stress changes imparted by nearby deformation events, including other earthquakes and aseismic processes, such as fault creep and postseismic relaxation. The Hayward fault (HF), undergoing both seismic and aseismic fault slip, provides a unique opportunity to study the mutual relation of seismic and aseismic processes on a fault system. We use surface deformation data obtained from InSAR (interferometric synthetic aperture radar), creepmeters and alinement arrays, together with constraints provided by repeating earthquakes to investigate the kinematics of fault creep on the northern HF and its relation to two seismic clusters ($M_w \leq 4.1$) in October 2011 and March 2012, and an M_w4.2 event in July 2007. Recurrences of nearby repeating earthquakes show that these episodes involved both seismic and aseismic slip. We model the stress changes due to fault creep and the recent seismic activity on the locked central asperity of the HF, which is believed to be the rupture zone of past and future M~7 earthquakes. The results show that the shallow fault creep stresses the major locked central patch at an average rate of 0.001-0.003 MPa/yr, in addition to background stressing at 0.01-0.015 MPa/yr. Given the time-dependent nature of the creep, occasional deviations from this stressing rate occur. We find that the 2011 seismic cluster occurred in areas on the fault that are stressed up to 0.01 MPa/yr due to aseismic slip on the surrounding segments, suggesting that the occurrence of these events was encouraged by the fault creep. Changes in the probability of major earthquakes can be estimated from the imparted stress from the recent earthquakes and associated fault creep transients. We estimate that the 1-day probability of a large event on the HF only increased by up to 0.18% and 0.05% due to the static stress increase and stressing rate change by the 2011 and 2012 clusters. For the July 2007 south Oakland event (M_w4.2) the estimated increase of short-term probabilities is 50%, highlighting the importance of short-term probability changes due to transient stress changes.

1-Introduction

Areas of high slip deficit on partially locked faults are likely initiation points of subsequent large earthquake ruptures (e.g. (Konca et al., 2008; Moreno et al., 2001; Uchida and Matsuzawa, 2011)). Identifying such strongly coupled areas helps to constrain the timing, extent and magnitudes of a future event (e.g. (Chlieh et al., 2008; Fialko, 2006; Manaker et al., 2003; Schmidt et al., 2005)). Smaller locked asperities may break more frequently during lower-magnitude events (e.g. (Nadeau and McEvilly, 1999; Nadeau and McEvilly, 2004; Vidale et al., 1994)). While these smaller earthquakes don't generate significant ground shaking, they, together with associated slow-slip transients, may modify the short-term probability of rupture of larger nearby sections of the fault exposed to transient stress increases (e.g. (Mazzotti and Adams, 2004)). For instance, the large Tohoku 2011 event

(M_w9) was preceded by 51 hours by a smaller foreshock and associated slow slip, which suggests a triggering relationship (Kato et al., 2012; Ohta et al., 2012). Therefore, characterizing the relation of seismic and aseismic slip episodes to major locked zones is of great importance for time-dependent operational earthquake forecasting (Jordan and Jones, 2010).

The HF has distinct types of activity, including coseismic ruptures (such as a M_w6.8 earthquake in 1868), aseismic creep and abundant microseismicity (e.g. (Lienkaemper et al., 1991; Schmidt et al., 2005; Toppozada and Borchardt, 1998; Waldhauser and Ellsworth, 2002)). The 1868 earthquake likely involved rupture of a large locked section of the fault extending from Oakland to near Fremont below a zone of shallow creep in the upper 3-5 km (e.g., (Lienkaemper et al., 2012; Schmidt et al., 2005; Shirzaei and Bürgmann, 2013)). The mean probability for $M \geq 6.7$ events on the Hayward-Rodgers Creek fault zone in the next 30 years is 31% (Working Group on California Earthquake Probabilities, 2011). This estimate, however, does not consider the effects of the transient changes of fault creep rates and may be modified temporally due to interaction with neighboring systems (e.g. (Parsons, 2002; Pollitz et al., 2004)).

On October 2011 (O11) and March 2012 (M12), two seismic clusters struck the northern part of the HF 5-20 km SE of Pt. Pinole (Fig. 1a). Figure (1a) shows the location and rupture areas of these seismic clusters and the July 20, 2007 south Oakland M_w4.2 event, which we discuss later. Figure (1b) also presents the spatio-temporal evolution of the O11 swarm showing a northward migration of seismicity along the HF. The O11 swarm includes 18 events $0.7 \leq M_w \leq 4.0$ that occurred over a span of 10 days (http://ddrt.ldeo.columbia.edu/DDRT/specevents/2011_M4.0_Berkeley/). Assuming a 3-MPa stress drop, the associated rupture area of the largest event is 1.1 km^2. In contrast to the O11 swarm, the M12 cluster includes a mainshock, immediately preceded by a M_w3.5 foreshock and followed by several aftershocks. The mainshock (M_w4.1) ruptured an area of ~2 km^2. As described below, we find that several aftershocks of the two clusters represent repeats of prior failures of the same slip patches, suggesting rapid nearby fault creep (e.g. (Nadeau and McEvilly, 1999)).

This section of the HF (0-20km) experienced only 10 M > 3.5 events since 1950, according to the ANSS catalog (Advanced National Seismic System). Given the empirical probability that earthquakes in California have a ~5% chance to be foreshocks of subsequent larger events within several days (Reasenberg and Jones, 1989), and the location of the events close to the main locked zone of the HF at depth (Schmidt et al., 2005), the multiple felt events caused concern both in the local communities and among researchers.

In this study we investigate the relation between the subsurface kinematics of HF creep rate, the source locations of the recent seismic clusters and their afterslip zones, and we present estimates of changes in large-earthquake probabilities due to the recent activity. To this end, we employ a joint inverse modeling approach and combine the deformation data from interferometric processing of a large SAR data set, surface creepmeters and alinement arrays (Shirzaei and Bürgmann, 2013). Then we calculate the static stress imparted on the primary HF asperity from creep and seismic events and the stressing rate change due to the O11 swarm, and further investigate them in a probabilistic framework to obtain estimates of the short-term probability change for a large event on the HF. We also used repeating earthquakes to estimate pre- and postseismic transient creep associated with the O11 cluster. Our results show that 1) the long-term creep induced stress encouraged occurrence of the O11 and M12 events, 2) some of the events associated with the 2011 and 2012 clusters represent repeaters revealing increased creep rates and associated stress changes, 3) constraints from repeaters help resolve the asperities associated with such deep seismic events and associated aseismic slip, 4) the recent seismic events caused accelerated creep and transient changes of the short-term earthquake probability on nearby locked fault segments in the following days.

2- Methods

2-1- Repeating earthquakes along the northern Hayward fault

Along the northern HF (0 – 40 km from Pt Pinole), we expand the repeating earthquake catalog of *Schmidt, et al.* (2005) down to magnitude ~0, by making use of borehole seismic data recorded at the Northern HF Network (NHFN) stations from microearthquakes that occurred from July 1995 to July 2012. The NHFN stations are equipped with three-component geophones and accelerometers at a depth of 30 to 200 m and the waveform data are sampled at 500 samples per second (Uhrhammer and McEvilly, 1997).

Following Schmidt, et al. (2005), we use a waveform cross-correlation approach with a 5.12-sec time window beginning with the first *P*-phase arrival. This time window typically includes the direct *S*-wave and *S*-coda. We evaluate the waveform similarity for a pair of seismograms in the vertical component with an 8-24 Hz bandpass filter based on the waveform cross-correlation coefficient and the phase coherency. To minimize the false detection of repeating earthquakes, we identify a pair of earthquakes as repeaters if both cross-correlation coefficient and the coherency are greater than 0.95. Our cross-correlation and coherency thresholds are comparable to those used in previous studies (e.g., (Peng and Zhigang, 2009; Templeton et al., 2009)).

Another approach to identify the repeating earthquakes is to explore the distances between pairs of earthquakes. To this end we use the earthquake catalog obtained following double-difference relocating approach (Waldhauser and Ellsworth, 2002) and use the assumption of a circular fault model (Eshelby, 1957) with a 3 MPa stress drop. As seen in Figure (S1), this approach identifies several non-repeating earthquakes, which appear their estimated rupture area overlaps significantly with that of surrounding events. Thus, the direct use of the inter-events distance does not reliably identify the repeating events.

6 April 2009 L'Aquila earthquake (Mw=6.3), which was preceded by several months of elevated seismicity (Jordan and Jones, 2010; Papadopoulos et al., 2010). Here we estimate changes in probability of a major Hayward fault earthquake on the primary locked rupture asperity caused by 1) small step-like static stress changes from nearby seismic and aseismic slip events, and 2) temporary stressing rate changes due to a seismic swarm. The probability that an earthquake occurs in the time T inside the interval $\left[t,\, t+\Delta t\right]$ is (e.g. (Working Group on California Earthquake Probabilities, 2011))

$$P(t \le T \le t+\Delta t) = \int_{t}^{t+\Delta t} f(t)dt \quad , \quad P(t \le T \le t+\Delta t \mid T > t) = \frac{P(t \le T \le t+\Delta t)}{P(t \le T < \infty)} \qquad (4)$$

In this study $f(t)$ is a Brownian Passage Time defined as (Meyer, 1970);

$$f(t,t_r,\alpha) = \sqrt{\frac{t_r}{2\pi\alpha^2 t^3}}\exp\left(-\frac{(t-t_r)^2}{2t_r\alpha^2 t}\right) \qquad (5)$$

where t_r and α are the average earthquake repeat time and aperiodicity, respectively. For the HF, we adopted values of 161 years and 0.4, respectively, determined from paleoseismic studies by (Lienkaemper et al., 2010). A positive Coulomb failure stress change (Ў# &) 3 causes a clock advance, which can be estimated through Ўۦ پ ۛ / ۛ, where 4ج is the tectonic stressing rate (0.01 - 0.015 MPa/yr after Parsons (2002)). To update the earthquake probability due to the imparted static stress, the clock advance can be used to adjust the elapsed time since the last event or alternatively to adjust the length of the earthquake recurrence interval (Parsons, 2005). Small stress changes from creep transients and nearby earthquakes are common and make up a fraction of the total stress increase during each Hayward fault earthquake recurrence interval. Thus, the mean repeat time of large events on the Hayward is not likely to change due to these small stress increments and we use the former strategy and adjust the time since the last earthquake to estimate the corresponding change in earthquake probability. Using this approach, the permanent probability change is most significant at the time of the stress increment, and then slowly approaches the unchanged maximum probability value with time (Parsons, 2005).

In addition to the permanent probability change, the imparted ΔCFS causes a transient change in the earthquake probability, which can be evaluated using a rate-state friction law (Working Group on California Earthquake Probabilities, 2011). Given the temporary increase in the rate of seismicity due to the imparted stress, the earthquake occurrence can be represented as a non-stationary Poisson process. Accordingly, the probability of an earthquake occurring in the interval $[t, t+\Delta t]$ is given by (Working Group on California Earthquake Probabilities, 2011);

(6)

where is the time-dependent seismicity rate (Dieterich, 1994) and ű ò is the expected number of earthquakes in the interval Ўò Integrating following a stress step for the interval to yields (Working Group on California Earthquake Probabilities, 2011);

(7)

ȍ ” ″Y

In Equation 7, is the seismicity rate associated with the permanent effect of the stress change, is a fault constitutive parameter, is the effective normal stress, is the duration of transient effects (here, 10 years after Parsons (2005)) and is the conditional probability

the gap and released part of the slip deficit. The largest M_w 4 event of the M12 cluster ruptured an area of ~2 km^2, where the creep model suggests ~8 mm/yr of creep. Given the long term slip rate of ~9 mm/yr (e.g. (Lienkaemper et al., 1991)), our model would suggest that this area did not accumulate significant slip deficit.

4- Discussion

Here we investigate the kinematics of creep rate between 1992 and 2010 on the HF and its relation to the significant seismic clusters in 2011 and 2012 and the major locked section representing likely future ~M7 rupture zones. To this end we use joint inversion of the deformation data obtained from InSAR, creepmeter and alinement arrays and focus on the two seismic clusters in October 2011 and March 2012 along the northern Hayward fault. Though we are able to resolve a ~6-km-deep locked patch near the source area of the O11 cluster, due to poor coverage of the geodetic data and lack of resolution at depth, the rupture area of the M12 events was not recognized to be locked in the slip model.

We examine whether our kinematic model is able to resolve the asperity that ruptured during the M12 seismic events or a larger locked zone proposed by Waldhauser and Ellsworth (2002). Based on the distribution of microseismicity, Waldhauser and Ellsworth, (2002) speculated that the HF is locked from 5 to 25 km distance and depth of 6-9 km (see Figure 10 of (Waldhauser and Ellsworth, 2002)). To test this scenario, we repeat the inversion but this time we impose a zero-slip constraint on the patches from km 5 – 25 and depth range of 6 – 9 km (Fig. 3c). Figure (3d) shows the difference between the modeled surface deformation obtained by the constrained (Fig. 3c) and unconstrained (Fig. 3a) creep rate inversion. The maximum difference is ~ 0.1 mm/yr, suggesting that even a larger locked patch as suggested by Waldhauser and Ellsworth (2002) cannot be ruled out by the data. Thus, we conclude that the lack of resolution does not allow resolving such details at depths of 6-9 km or greater.

Our updated catalogue of repeating earthquakes (Table A1 and purple dots in Fig. 3a) includes several events within the proposed locked zone of Waldhauser and Ellsworth (2002). This suggests that the extent of any locked zone would be smaller than they envisioned.

To investigate the relationship between the distribution of creep rate, the seismic clusters and the primary locked asperity along the HF, we calculate the Coulomb Failure Stress change (Ўő ̏Ο) ̏(King et al., 1994) induced by the creep on the HF using the creep rate model shown in Figure (3a). Figure (4) shows the distribution of the aseismic Ўő ̏Ο ̏rate. The fault creep imparts stress at rates of 0.001-0.003 MPa/yr on the main locked zone along the central part of the fault. This stress is in addition to that induced by shearing at the plate boundary estimated at 0.01-0.015 MPa/yr (Parsons, 2002). There is another smaller zone of increasing stress along the northern HF, which receives up to 0.01 MPa/yr Ўő ̏Ο ̏in addition to the background stressing rate. The O11 cluster is near these stressed patches, suggesting that the HF creep has enhanced occurrence of this event.

The probability of large seismic events on the HF may vary through interaction with other faults and due to slip events on the HF near the major locked asperity. For example, the stress shadow caused by the 1906 M7.8 San Francisco earthquake yields a 7-12% reduction of the 30-years probability of a large HF rupture calculated for 2002, compared to estimates without this contribution (Parsons, 2002). Taking into account the effect of time-dependent interseismic strain accumulation, coseismic strain release, and viscoelastic relaxation, as well as the uncertainty of the mean repeat time, Pollitz and Schwartz (2008) estimate a 30-year probability of 40% - 70% for a rupture of the HF, much larger than the 31% suggested by Working Group on California Earthquake Probabilities (2011). In addition to stress changes due to regional events, small nearby slip events on the HF may change the loading on the locked zone, and consequently the short-term probability of a future earthquake.

To evaluate short-term changes in earthquake hazard caused by slow slip and tremor events down-dip of the locked section of the Cascadia subduction zone, Mazzotti and Adams, (2004) calculate substantially increased probabilities (by a factor of 30-100) of major earthquakes due to the associated increases of stress during the ~two-week-long events. Similarly, small earthquakes and silent slip events near the locked section of the HF may lead to changes in short-term earthquake probabilities. To evaluate the permanent and transient probability changes caused by step-like changes in the stress field and the gradual changes in the tectonic stressing rate due to O11 and M12 events and associated creep transients, we use the framework detailed in section 2.4 and the Matlab scripts in the Auxiliary Material. The results show that the 1-day probability of a large event on the north Hayward changes by only 0.18% and 0.05% due to step-like peak stress changes of 0.2 and 0.05 kPa on the locked zone from the O11 and M12 events, respectively. These small stress changes correspond to clock advances of only 6 days and 1.5 days, which are used to adjust the elapsed time since the last earthquake in the calculation of the permanent probability change. The permanent probability increases estimated from these small static stress changes are even smaller; 0.01% and 0.003%, respectively.

The above calculation only considers the effects of the largest events in each cluster. However, swarms and associated slow slip, such as that of O11, impart stress gradually and also cause changes in the stressing rate. The associated 1-day probability change for the O11 swarm is 0.015%, which is much smaller than the probability change due to step-like stress increase. For this estimation the aftershock duration following the seismic swarm is estimated to be 100 days (see Figure S2). Note that the estimate of the transient effect increases when considering the contributions of aseismic slip indicated by the repeaters (see below). These are very small changes compared to that caused by the M_w4.2 July 20, 2007 south Oakland event located closer to the primary HF asperity (yellow circle in Figs. 1a and 3). The estimated transient 1-day probability change for this event is 50%.

To characterize possible changes in HF creep rate prior to and after the O11 seismic cluster, we use the repeating earthquake sequences in the vicinity of the O11 and M12 episodes, identified since 1995 (Table S1, Fig. 5a). Figure (5b) shows the sequence of repeaters along the northern HF and vertical lines connect the members of a repeating cluster. Applying the method to estimate cumulative slip from a population of repeating sequences detailed in Nadeau and McEvilly, (2004) and a moving average window of 100 days, we obtain the creep rate shown in Figure (5c) for the area of O11, highlighted in Figure (5b). Our analysis identifies three repeating earthquakes around 150 days before the O11 mainshock, suggesting an increase in creep rate from 5 mm/year to 10 mm/year. Additionally, there is a marked increase of creep rate following the mainshock for about 100 days. The cumulative slip during this 100-day period is estimated at 26 mm. While we do not know the full extent of the slow-slip zone, aseismic creep would have contributed the equivalent moment of a M_w 4.17 earthquake if we assume a 3x1 km slip zone. Thus, stress and probability changes from O11 afterslip approximately doubled the seismic contribution.

In summary, this study highlights the importance of small nearby seismic and aseismic slip events in changing the short-term probability of a major seismic event, if they occur very close to major locked rupture asperities. Quantification of time-dependent hazard due to such transient stress changes is an important goal of operational earthquake forecasting approaches currently being considered (Jordan and Jones 2010). Future implementation of operational earthquake forecasting could rely on a combination of such models of fault interaction and statistical approaches to estimate, and communicate to the public, short-term changes in earthquake hazard. In the light of these results one can establish a scientific base assisting authorities to deal with cases similar to the L'Aquila event, where elevated seismicity rates were observed in an area of high seismic hazard, but no formal reevaluation of earthquake probability was undertaken.

5- Conclusions

We investigate the relation between the HF creep, locked asperities and recent seismic clusters that occurred on October 2011 and March 2012 along the northern HF. We jointly invert InSAR and surface creep data for the distribution of sub-surface creep along the HF. We identify a ~20-km-long primary locked zone below ~5 km depth along the central HF, which may represent the rupture zone of past and future major earthquakes, as well as smaller-scale variations in creep rate at depth. Simple resolution tests show that we cannot uniquely resolve smaller features at the scale of the recent O11 and M12 failures from the geodetic data. Repeating microearthquakes provide additional constraints on the location and rates of creep at depth. We find that the location of the seismic clusters is adjacent to areas that are stressed due to fault creep, suggesting that these events were triggered by the stress induced by aseismic slip on nearby sections of the fault. Following Toda, et al. (1998), we estimate that the O11, M12 and July 2007 south Oakland events changed the short-term 1-day probability of a major earthquake on the HF by 0.15%, 0.04% and 45%, respectively. This, however, is an underestimate of the probability change, as we did not consider the effect of aseismic slip triggered by these events. For the O11 sequence, the equivalent moment of the triggered aseismic slip is equivalent to an M_w4.17, thus nearly doubling stress and probability estimates. We conclude that consideration of small seismic events and aseismic slip transients near major locked zones of partially coupled faults as precursor candidates is of importance for operational earthquake forecasting efforts characterizing time-dependent earthquake hazard.

6- References

Bilham, R. and Whitehead, S., 1997. Subsurface creep on the Hayward fault, Fremont, California. Geophys. Res. Lett., 24(11): 1307-1310.

Bjerhammar, A., 1973. Theory of errors and generalized matrix inverse. Elsevier publishing company, Amsterdam, 127-128 pp.

Bürgmann, R., Hilley, G., Ferretti, A. and Novali, F., 2006. Resolving vertical tectonics in the San Francisco Bay Area from permanent scatterer InSAR and GPS analysis. Geology, 34(3): 221-224.

Chen, C.W. and Zebker, H.A., 2001. Two-dimensional phase unwrapping with use of statistical models for cost functions in nonlinear optimization. J. Opt. Soc. Am. A., 18: 338–351.

Chlieh, M., Avouac, J.P., Sieh, K., Natawidjaja, D.H. and Galetzka, J., 2008. Heterogeneous coupling of the Sumatran megathrust constrained by geodetic and paleogeodetic measurements. Journal of Geophysical Research-Solid Earth, 113(B05305): doi:10.1029/2007JB004981.

Dieterich, J.H., 1994. A constitutive law for rate of earthquake production and its application to earthquake clustering. J. Geophys. Res., 99: 2601-2618.

Eshelby, J.D., 1957. The determination of the elastic field of an ellipsoidal inclusion, and related problems. Proc. R. Soc. London, 241: 376-396.

Ferretti, A., Prati, C. and Rocca, F., 2001. Permanent scatterers in SAR interferometry. IEEE transactions on geoscience and remote sensing, 39: 8-20

Fialko, Y., 2006. Interseismic strain accumulation and the earthquake potential on the southern San Andreas fault system. Nature, 441(7096): 968-971.

Franceschetti, G. and Lanari, R., 1999. Synthetic aperture radar processing. CRC Press.

Funning, G.J., Burgmann, R., Ferretti, A. and Novali, F., 2007. Asperities on the Hayward fault resolved by PS-InSAR, GPS and boundary element modeling. Eos Trans. AGU 88(52).

Jordan, T.H. and Jones, L.M., 2010. Operational Earthquake Forecasting: Some Thoughts on Why and How. Seismological Research Letters, 81(4): 571-574.

Kato, A., Obara, K., Igarashi, T., Tsuruoka, H., Nakagawa, S. and Hirata, N., 2012. Propagation of Slow Slip Leading Up to the 2011 M-w 9.0 Tohoku-Oki Earthquake. Science, 335(6069): 705-708.

King, G.C.P., Stein, R.S. and Lin, J., 1994. Static stress changes and the triggering of earthquakes. Bull. Seism. Soc. Am., 84: 935-953.

Konca, A.O., Avouac, J.P., Sladen, A., Meltzner, A.J., Sieh, K., Peng, F., Zhenhong, L., Galetzka, J., Genrich, J., Chlieh, M., Natawidjaja, D.H., Bock, Y., Fielding, E.J., Chen, J. and Helmberger, D.V., 2008. Partial rupture of a locked patch of the Sumatra megathrust during the 2007 earthquake sequence. Nature, 456(7222).

Lienkaemper, J.J., Borchardt, G. and Lisowski, M., 1991. Historic creep rate and potential for seismic slip along the Hayward Fault, California. J. Geophys. Res., 96: 18261-18283.

Lienkaemper, J.J. and Galehouse, J.S., 1997. Revised long-term creep rates on the Hayward fault, Alameda and Contra Costa counties, California, U.S. Geol. Surv.

Lienkaemper, J.J., McFarland, F.S., Simpson, R.W., Bilham, R.G., Ponce, D.A., Boatwright, J.J. and Caskey, S.J., 2012. Long-Term Creep Rates on the Hayward Fault: Evidence for Controls on the Size and Frequency of Large Earthquakes. Bulletin of the Seismological Society of America, 102(1): 31-41.

Lienkaemper, J.J., Williams, P.L. and Guilderson, T.P., 2010. Evidence for a Twelfth Large Earthquake on the Southern Hayward Fault in the Past 1900 Years. Bulletin of the Seismological Society of America, 100(5A): 2024-2034.

Manaker, D.M., Burgmann, R., Prescott, W.H. and Langbein, J., 2003. Distribution of interseismic slip rates and the potential for significant earthquakes on the Calaveras fault, central California. Journal of Geophysical Research-Solid Earth, 108(B6): 2287, doi:2210.1029/2002JB001749.

Mazzotti, S. and Adams, J., 2004. Variability of near-term probability for the next great earthquake on the Cascadia Subduction zone. Bull. Seism. Soc. Am., 94(5): 1954-1959.

Meyer, P.L., 1970. Introductory Probability and Statistical Applications. oxford & IBH 367 pp.

Mikhail, E.M., 1976. Observations and least squares IEP New York, 497 pp.

Moreno, Y., Correig, A.M., Gómez, J.B. and Pacheco, A.F., 2001. A model for complex aftershock sequences. Journal of Geophysical Research, 106: 6609-6619.

Nadeau, R.M. and McEvilly, T.V., 1999. Fault slip rates at depth from recurrence intervals of repeating microearthquakes. Science, 285(5428): 718-721.

Nadeau, R.M. and McEvilly, T.V., 2004. Periodic pulsing of characteristic microearthquakes on the San Andreas fault. Science, 303(5655): 220-222.

O'leary, D.P., 1990. Robust Regression Computation Using Iteratively Reweighted Least-Squares. Siam Journal on Matrix Analysis and Applications, 11(3): 466-480.

Ohta, Y., Hino, R., Inazu, D., Ohzono, M., Ito, Y., Mishina, M., Iinuma, T., Nakajima, J., Osada, Y., Suzuki, K., Fujimoto, H., Tachibana, K., Demachi, T. and Miura, S., 2012. Geodetic constraints on afterslip characteristics following the March 9, 2011, Sanriku-oki earthquake, Japan. Geophysical Research Letters, 39: doi:10.1029/2012GL052430.

Papadopoulos, G.A., Charalampakis, M., Fokaefs, A. and Minadakis, G., 2010. Strong foreshock signal preceding the L'Aquila (Italy) earthquake ($M_{\rm w}$similar to 6.3) of 6 similar to April similar to 2009. Natural Hazards and Earth System Sciences, 10(1): 19-24.

Parsons, T., 2002. Post-1906 stress recovery of the San Andreas fault system calculated from three-dimensional finite element analysis. J. Geophys. Res., 107(B8): 1-13.

Parsons, T., 2005. Significance of stress transfer in time-dependent earthquake probability calculations. J. Geophys. Res., 110(B5): 1-20, doi: 10.1029/2004JB003190.

Peng, Z. and Zhigang, P., 2009. Depth extent of damage zones around the central Calaveras fault from waveform analysis of repeating earthquakes. Geophysical Journal International, 179(3).

Pollitz, F., Bakun, W.H. and Nyst, M., 2004. A physical model for strain accumulation in the San Francisco Bay region: Stress evolution since 1838. J. Geophys. Res., 109(B11): doi: 10.1029/2004JB003003.

Pollitz, F.F. and Schwartz, D.P., 2008. Probabilistic seismic hazard in the San Francisco Bay area based on a simplified viscoelastic cycle model of fault interactions. Journal of Geophysical Research-Solid Earth, 113(B5).

Reasenberg, P.A. and Jones, L.M., 1989. Earthquake hazard after a mainshock in California. Science, 243: 1173-1176.

Schmidt, D.A., Bürgmann, R., Nadeau, R.M. and d'Alessio, M., 2005. Distribution of aseismic slip rate on the Hayward fault inferred from seismic and geodetic data. J. Geophys. Res., 110(B8): doi: 10.1029/2004JB003397.

Segall, P. and Harris, R., 1987. The earthquake deformation cycle on the San Andreas fault near Parkfield, California. J. Geophys. Res., 92: 10511-10525.

Shirzaei, M., 2013. A Wavelet-Based Multitemporal DInSAR Algorithm for Monitoring Ground Surface Motion. Ieee Geoscience and Remote Sensing Letters, 10(3): 456-460.

Shirzaei, M. and Bürgmann, R., 2012. Topography correlated atmospheric delay correction in radar interferometry using wavelet transforms. Geophysical Research Letters, 39(1): doi: 10.1029/2011GL049971.
Shirzaei, M. and Bürgmann, R., 2013. Time-dependent model of creep on Hayward fault inferred from joint inversion of 18 years InSAR time series and surface creep data. JGR: doi:10.1029/2012JB009497R, in press.
Shirzaei, M. and Walter, T.R., 2011. Estimating the effect of satellite orbital error using wavelet based robust regression applied to InSAR deformation data. IEEE Transactions on Geoscience and Remote Sensing, 49(1): 4600 - 4605.
Templeton, D.C., Nadeau, R.M. and Bürgmann, R., 2009. Distribution of postseismic slip On the Calaveras fault, California, following the 1984 M6.2 Morgan Hill earthquake. Earth and Planetary Science Letters, 277(1-2): 1-8.
Toda, S., Stein, R.S., Reasenberg, P.A., Dieterich, J.H. and Yoshida, A., 1998. Stress transferred by the 1995 Mw=6.9 Kobe, Japan, shock: Effects on aftershocks and future earthquake probabilities. Journal of Geophysical Research, 103(B10): 24543-24565.
Toda, S., Stein, R.S. and Sagiya, T., 2002. Evidence from the AD 2000 Izu islands earthquake swarm that stressing rate governs seismicity. Nature, 419(6902): 58-61.
Toppozada, T.R. and Borchardt, G., 1998. Re-evaluation of the 1836 "Hayward fault" and the 1838 San Andreas fault earthquakes. Bulletin of the Seismological Society of America, 88(1): 140-159.
Uchida, N. and Matsuzawa, T., 2011. Coupling coefficient, hierarchical structure, and earthquake cycle for the source area of the 2011 off the Pacific coast of Tohoku earthquake inferred from small repeating earthquake data. Earth Planets and Space, 63(7): 675-679.
Uhrhammer, R.A. and McEvilly, T.V., 1997. Performance of a borehole network in an urban environment; the Hayward Fault network. Seismological Research Letters, 68(2): 332.
Vidale, J.E., Ellsworth, W.L., Cole, A. and Marone, C., 1994. Variations in Rupture Process with Recurrence Interval in a Repeated Small Earthquake. Nature, 368(6472): 624-626.
Waldhauser, F. and Ellsworth, W.L., 2002. Fault structure and mechanics of the Hayward Fault, California, from double-difference earthquake locations. J. Geophys. Res., 107(3): ESE 3-1 to ESE 3-15.
Waldhauser, F., Ellsworth, W.L. and Cole, A., 1999. Slip-parallel seismic lineations on the northern Hayward fault, California. Geophysical Research Letters, 26(23): 3525-3528.
Working Group on California Earthquake Probabilities, 2011. The Uniform California Earthquake Rupture Forecast, Version 3 (UCERF3) Project Plan, U. S. Geological Survey.

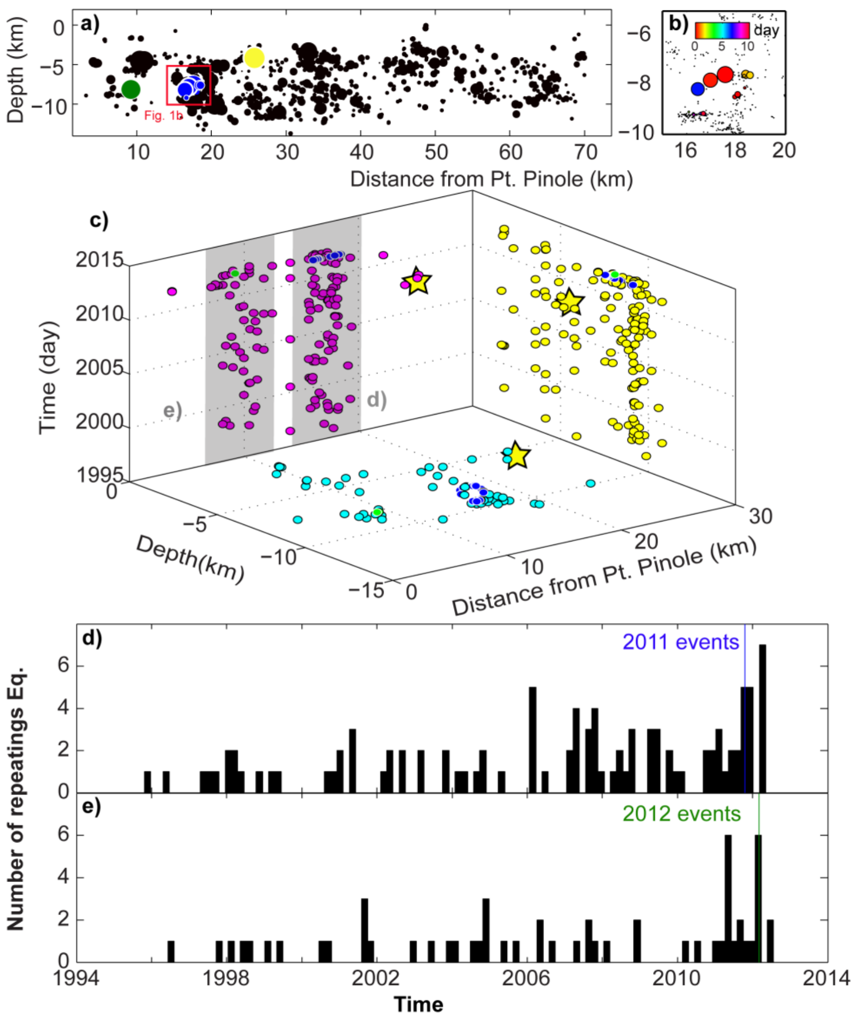

Figure 1: a) Relocated microseismicity (black circles, obtained from http://www.ldeo.columbia.edu/~felixw) along the Hayward fault. The October 2011 (O11), March 2012 (M12), and the July 20, 2007 M_w4.2 south Oakland earthquakes are shown by blue, green and yellow circles, respectively. Note that the M12 events are precisely collocated, therefore, only one event is seen. b) Spatio-temporal evolution of the October 2011 seismic swarm. The symbol colors reflect the relative timing of events as indicated by the inset color scale c) The catalog of repeating earthquakes for the past 17 years at the northern Hayward fault including repeating events participating in the O11 (blue circles) and M12 (green circles) clusters. The yellow star presents the July 20, 2007 M_w4.2 event. d, e) 100-day bin histogram of repeating earthquakes for the areas marked in panel (1c). Vertical blue and green lines indicate timing of O11 and M12 seismic clusters.

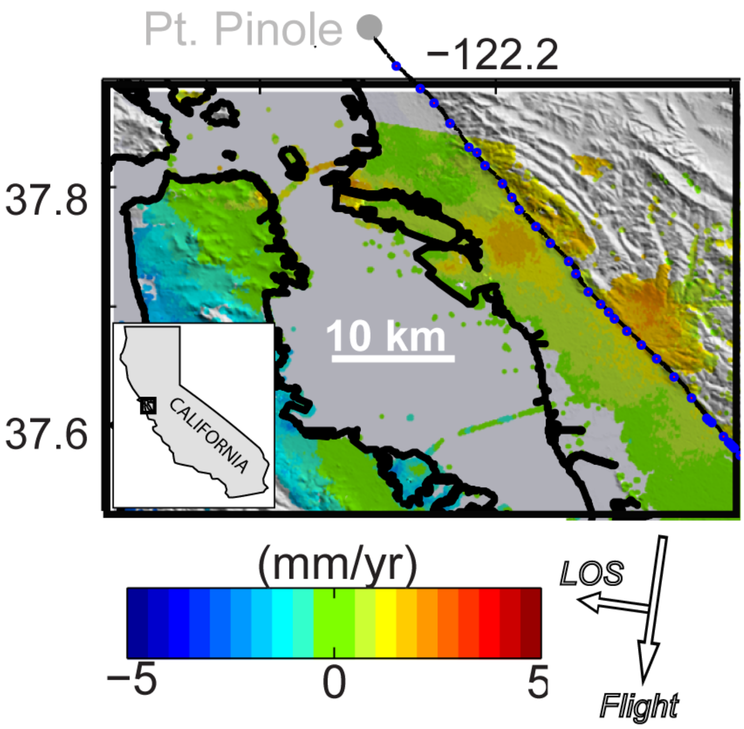

Figure 2: LOS velocity map over the northern Hayward fault. Warmer colors represent motions toward the satellite (incidence angle = 23°, heading angle = 188°). The trace of the Hayward fault (black line) and the location of creepmeters and alinement arrays (blue dots) are shown. InSAR time series method and data used to obtain the LOS velocities are from Shirzaei and Bürgmann (2013).